

Future increases in Amazonia water stress from CO₂ physiology and deforestation

Received: 15 November 2022

Accepted: 3 August 2023

Published online: 31 August 2023



Yue Li¹✉, Jessica C. A. Baker², Paulo M. Brando^{3,4}, Forrest M. Hoffman⁵, David M. Lawrence⁶, Douglas C. Morton⁷, Abigail L. S. Swann^{8,9}, Maria del Rosario Uribe³ & James T. Randerson¹

Several different drivers are contributing to climate change within the Amazon basin, including forcing from greenhouse gases and aerosols, plant physiology responses to rising CO₂, and deforestation. Attribution among these drivers has not been quantified for Shared Socioeconomic Pathway (SSP) climate simulations. Here we identify the contribution of CO₂ physiology and deforestation to future hydroclimate change in the Amazon basin by combining information from four experiments and eight different Earth system models in Coupled Model Intercomparison Project Phase 6. Together, forcing from CO₂ physiology and deforestation account for about 44% of the projected annual precipitation decline, 48% of surface relative humidity decline and 11% of warming over the Amazon basin by 2100 for SSP3-7.0. Other Coupled Model Intercomparison Project Phase 6 SSP simulations have similar contributions from the two drivers. Insight from our attribution analysis can aid in identifying research priorities aimed at reducing uncertainty in future projections of water availability, carbon dynamics and wildfire risk.

Climate change is a major threat to Amazon rainforests as warming and drying contribute to higher levels of tree mortality in intact forests^{1,2} and to more destructive fires that escape human control^{3,4}. To explore both future climate change and its impacts within the Amazon basin, Earth system model (ESM) simulations from the 5th and the 6th Phases of the Coupled Model Intercomparison Project (CMIP)^{5–12} are widely used. Specifically, simulations from ScenarioMIP¹³ for different future Shared Socioeconomic Pathway (SSP)¹⁴ scenarios have been analysed extensively to assess climate change impacts on ecosystem composition¹⁵, carbon storage¹⁶, the hydrological cycle¹⁷, fire risk¹⁸ and socioeconomic systems¹⁹, often with the CMIP simulations serving as external forcing for a set of downstream models that resolve the basin with a higher spatial resolution or greater process representation (for example, ref. 16). Another important application of the CMIP simulations is their use in the development of emergent constraints²⁰, which

allow for a better understanding of the individual models from the broader ensemble that are more likely to accurately predict the sign and magnitude of future change^{21–23}. Despite the extensive use of SSP simulations for these purposes, we do not clearly understand how different forcing agents within the simulations contribute to projected future changes in climate and the hydrological cycle in the Amazon basin.

Identifying the forcing agents responsible for projected future changes in climate is important for identifying research priorities to reduce uncertainties in key model components. In CMIP6 SSP simulations, critical forcing agents include well-mixed greenhouse gases, aerosols and land use change. Particularly for the Amazon basin, it is well established that the surface evapotranspiration changes from plant stomatal responses to rising atmospheric CO₂ and deforestation are important drivers of the precipitation response^{24–29}, yet studies analysing SSP simulations may include an implicit assumption that

¹Department of Earth System Science, University of California, Irvine, CA, USA. ²School of Earth and Environment, Leeds University, Leeds, UK. ³Yale School of the Environment, Yale University, New Haven, CT, USA. ⁴Instituto de Pesquisa Ambiental da Amazônia, Brasília, Brazil. ⁵Climate Change Institute, Oak Ridge National Laboratory, Oak Ridge, TN, USA. ⁶National Center for Atmospheric Research, Boulder, CO, USA. ⁷NASA Goddard Space Flight Center, Greenbelt, MD, USA. ⁸Department of Atmospheric Sciences, University of Washington, Seattle, WA, USA. ⁹Department of Biology, University of Washington, Seattle, WA, USA. ✉e-mail: yue.li@uci.edu

most of the projected change in the basin is associated with the climate system response to radiative forcing from greenhouse gases and aerosols since these are the main forcing agents at a global scale (for example, ref. 12). To ensure a successful and informative assessment for policy- and decision-makers, it is essential to provide comprehensive reports on both the magnitude of climate change and its consequences. Additionally, it is crucial to clearly quantify the factors that contribute to future regional change. Failing to fully understand these key drivers hinders progress in reducing uncertainties within climate models³⁰.

Future precipitation changes in Amazonia will probably be influenced by increased atmospheric CO₂ and deforestation^{31,32}. The CO₂ impacts on Amazonian precipitation can be separated into radiative and plant physiological effects. The CO₂ radiative effect alters physical and dynamic processes, with regional Amazonian precipitation responding to large-scale thermodynamical adjustments of the ocean–atmosphere system, including the ‘wet regions getting wetter’ mechanism identified in past work^{33,34}. By contrast, the plant physiological effect in response to rising CO₂ is associated with a reduction in plant stomatal conductance and land surface evapotranspiration, which, in turn, influences boundary layer processes, the frequency of deep convection, and interactions with the tropical jet³⁵. Though sharing similar mechanisms of reducing surface evapotranspiration and boundary layer humidity, deforestation additionally increases surface albedo and reduces surface roughness, two processes that play major roles in altering precipitation patterns in various parts of the Amazon basin^{36–38}. Across the basin as a whole, it has been suggested that increasing the deforestation fraction may cause a linear decline in regional average precipitation³⁹ and that for some scenarios of future change, this decline in precipitation may be similar in magnitude to that caused by forcing from CO₂ physiology⁴⁰.

Despite well-understood mechanisms describing how CO₂ physiology^{25,35,40} and deforestation⁴¹ cause precipitation reductions, there remains a lack of comprehensive and quantitative understanding of how these forcing agents contribute to future rainfall and other climate variable changes in future (twenty-first century) simulations conducted as a part of ScenarioMIP for different SSPs. This attribution is challenging, in part because each SSP has a different level of atmospheric CO₂ and prescribed forest cover change. In this Article, we attribute changes in Amazonian precipitation, surface relative humidity (RH) and climate warming in the SSP simulations to forcings from CO₂ physiology and deforestation. For this purpose, we analysed idealized model simulations from two model comparison projects (MIPs) that were undertaken as a part of CMIP6 (Methods), namely the Coupled Climate–Carbon Cycle Model Intercomparison Project (C4MIP⁴²) and the Land-Use Model Intercomparison Project (LUMIP⁴³). Idealized experiments of the land surface response to rising CO₂ in C4MIP (known as the biogeochemically coupled or BGC simulations) and to deforestation in LUMIP enabled us to first quantify the climate response of Amazonia rainforest to these two mechanisms under uniform simulation protocols. We specifically analysed transient simulations from eight models participating in C4MIP and six models participating in LUMIP (Supplementary Tables 1 and 2). This analysis revealed that regional annual mean precipitation, surface RH and air temperature respond linearly to atmospheric CO₂ concentration and forest cover fraction in the Amazon basin. In a second step, we applied linear models of the climate response to the absolute change in CO₂ concentration or forest cover fraction to quantify the contribution of these mechanisms to climate change in the Amazon basin for different CMIP6 SSP simulations.

Isolating the climate response to rising CO₂ or deforestation

We find that for the influence of rising CO₂ on plant physiology, the models show a significant (and mostly linear) decline in mean annual precipitation of $-0.91 \pm 0.07\%$ ($P < 0.001$, *t*-test) for a CO₂ increase of

100 ppm (Fig. 1a). Multiplied by the quadrupling increase in CO₂ (that is, from 285 ppm to 1,140 ppm between last and first 20 years of the C4MIP BGC simulations) and a basin-wide mean annual precipitation climatology of 6.1 mm per day, this precipitation response to the CO₂ physiological forcing is equivalent to -0.47 mm per day, which is broadly consistent with estimates for this response from the mean of previous CMIP5 models (for example, -0.48 mm per day in Kooperman et al.²⁵). We also find that all of the individual CMIP6 models analysed here show a significant negative precipitation response to CO₂ physiological forcing (ranging from -0.5% to -1.6% per 100 ppm CO₂ increase), highlighting a reasonably coherent response of Amazonian precipitation to CO₂ physiological forcing within CMIP6 (Supplementary Table 2).

Deforestation also significantly decreases mean annual precipitation in the Amazon basin (Fig. 1b). The multi-model average response is $-1.0 \pm 0.3\%$ per 10% deforestation ($P < 0.001$), relatively linear, and equivalent to about 10% or -0.61 ± 0.18 mm per day for 100% (complete) deforestation of the whole basin. The magnitude of the multi-model average precipitation response from the fully coupled LUMIP simulations for complete deforestation is similar to a recent estimate of $-12 \pm 11\%$ (per 100% deforestation) derived from a meta-analysis synthesizing information from climate models with various degrees of ocean, ice and atmospheric coupling³⁹. Moreover, we find all models agree on the sign of the response, with their magnitude ranging from -0.15% to -2.3% in response to a 10% loss of forest cover, despite important structural differences in the CMIP6 models with respect to the representation of vegetation–hydrology coupling and biophysical responses to land use change^{28,29}.

Spatially, the precipitation response to forcing from a 100 ppm CO₂ increment is strongest in the north-eastern part of the basin (Fig. 2a), with a pattern consistent with previous reports³⁴. Whereas the climate response to the basin-wide 10% deforestation is strongest in central and western Amazonia, adjacent to the Andes Mountain range (Fig. 2b). Further, the CO₂ physiological forcing and deforestation also influence the seasonality of the precipitation response. Across the annual cycle, the CO₂ physiology impacts on precipitation are somewhat uniform when expressed as a per cent change. However, the precipitation response in the southeastern part of the basin is stronger towards the end of the dry season (August and September) than at the beginning of the dry season (June and July) (Supplementary Fig. 1). The negative precipitation response to deforestation appears to be most robust across the models during the wet season (December to May), although there is also a strong response and high level of agreement across models in the northern and eastern part of the basin during August, September and October (Supplementary Fig. 2).

The negative precipitation response to forcing from CO₂ physiology and deforestation implies a greater future risk for meteorological drought and fire. To provide more insight into potential changes in these risks caused by CO₂ physiology and deforestation forcing, we performed a similar regression analysis (Methods) for surface RH from the five models with available output from C4MIP and the four models with available output from LUMIP. Basin-wide RH decreases at a rate of $-0.91 \pm 0.02\%$ ($P < 0.001$) in response to a 100 ppm CO₂ increase and by $-0.5 \pm 0.1\%$ ($P < 0.001$) in response to a 10% loss of tree cover in the Amazon basin (Fig. 1c,d). Regressions for each available model also confirm that the RH response is consistently negative in response to these drivers, although not every model exhibits a statistically significant trend (Supplementary Table 2). The spatial pattern of RH response to CO₂ physiology and deforestation is more homogeneous than the one for precipitation, with the largest signal occurring in the central Amazon basin (Supplementary Fig. 3a,b).

Similar to precipitation and RH, the surface air temperature response in the Amazon basin to forcing from CO₂ physiology is mostly linear (Fig. 1e), with a regional average warming rate of 0.13 ± 0.01 °C per 100 ppm increase in CO₂ ($P < 0.001$). All models agree on a significantly positive surface air temperature response to rising CO₂ (Supplementary

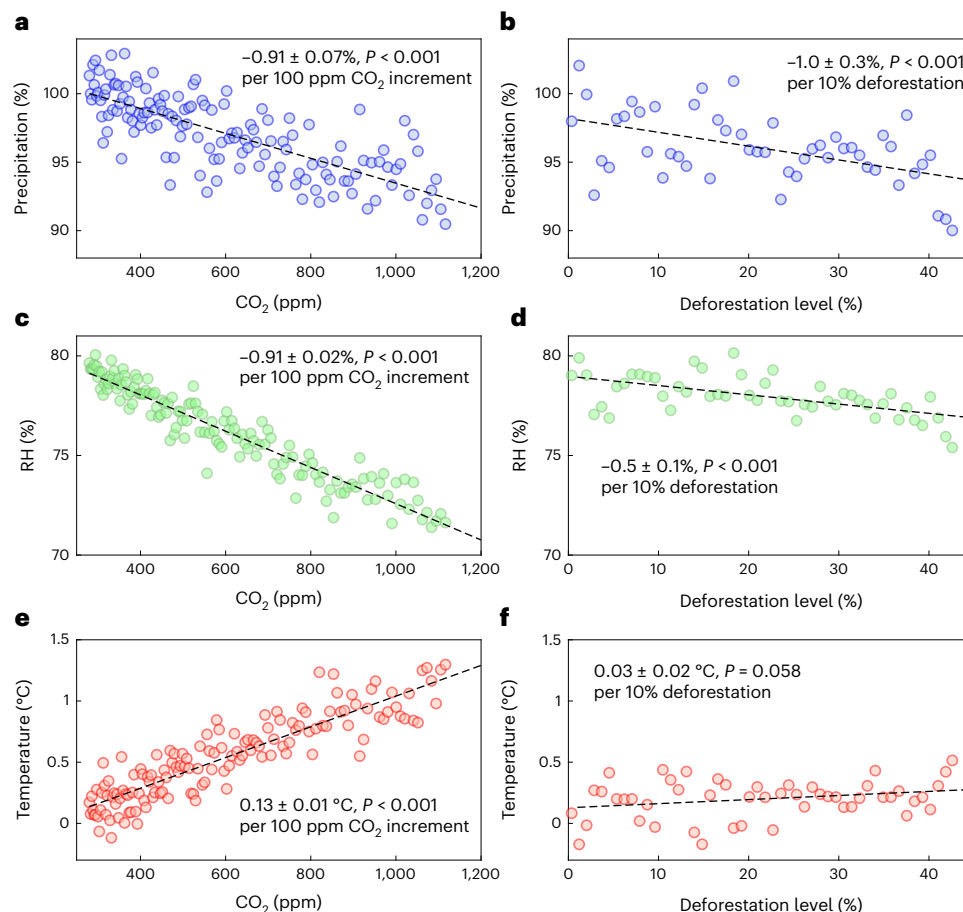


Fig. 1 | Transient response of annual mean precipitation, surface RH and air temperature to CO₂ physiology and deforestation in the Amazon basin.

a–f, The precipitation changes were computed in percentage from each model, and then averaged across eight CMIP6 models. Each data point represents the cross-model regional average computed for each year from their 140 year and

50 year simulations from the C4MIP and LUMIP experiments, respectively (Methods). Climate changes are solely due to CO₂ physiology (no radiative effects) in the left column and deforestation in the right column. The exact P values for regression slope by t -test are 4.5×10^{-28} (**a**), 2.1×10^{-4} (**b**), 8.8×10^{-73} (**c**), 6.0×10^{-6} (**d**), 9.4×10^{-51} (**e**) and 0.058 (**f**).

Table 2). This warming signal is likely to increase the water saturation vapour pressure, which, combined with the declined surface moisture availability due to declining stomatal conductance, contributes to the RH decline observed in the models for CO₂ physiology.

The surface air temperature response to deforestation is considerably noisier than for the other climate variables shown in Fig. 1f, with a 10% loss in forest fraction contributing to a basin-wide warming of $0.03 \pm 0.02\text{ }^{\circ}\text{C}$ ($P = 0.058$). Further regression analysis was performed for each model, revealing that the sign and magnitude of deforestation impact on surface air temperature diverge considerably from model to model ($-0.19\text{ }^{\circ}\text{C}$ to $0.15\text{ }^{\circ}\text{C}$ in response to 10% deforestation; Supplementary Table 2). Specifically, CanESM2 and UKESM1 show decreases in surface air temperature from deforestation in contrast to the other models that show a warming trend (Supplementary Table 2). Some of this variation may be linked to cooling from deforestation in the extra-tropics in the LUMIP simulations²⁸. As a result, the mean estimate of climate warming from deforestation reported here is probably a lower bound and has a high level of uncertainty that is associated with model-to-model variability (for further information, see Discussion). Compared with the spatial pattern of the precipitation response, the spatial patterns for the warming response to CO₂ physiology and deforestation are diffuse and broadly similar, with the strongest response in the central part of the basin (Supplementary Fig. 3c,d).

The climate responses to CO₂ physiology and deforestation are not directly comparable in Figs. 1 and 2, with the slopes having

different units. However, we can compare relative impacts of the two drivers by specifying a fixed increment of atmospheric CO₂ and then identifying the equivalent level of deforestation necessary to generate the same magnitude of climate change. For precipitation, a 100 ppm CO₂ increase is equivalent to a 9% increase in deforestation in terms of generating an equivalent amount of climate change for the CMIP6 models analysed here. Similarly, for RH, a 100 ppm CO₂ increase is equivalent to an 18% increase in deforestation, and for temperature, a 100 ppm CO₂ increase is equivalent to a 43% increase in deforestation.

Contribution of CO₂ physiology and deforestation within SSPs

The analysis shown in Fig. 1 provides evidence that the climate response to atmospheric CO₂ concentration or deforestation is mostly linear in CMIP6 models for the domain of the Amazon basin. As a next step, we used these linear relationships to separately isolate climate change arising from these two drivers in widely used SSP scenarios¹³ by the end of the twenty-first century. We estimated their contributions as the product of the multi-model average climate response from Fig. 1 and the changes in future atmospheric CO₂ concentration or deforestation fraction from each SSP simulation (Fig. 3 and Methods). Contributions from CO₂ physiology and deforestation have yet to be systematically identified for ScenarioMIP SSP simulations that integrate the forcing from many different climate change drivers.

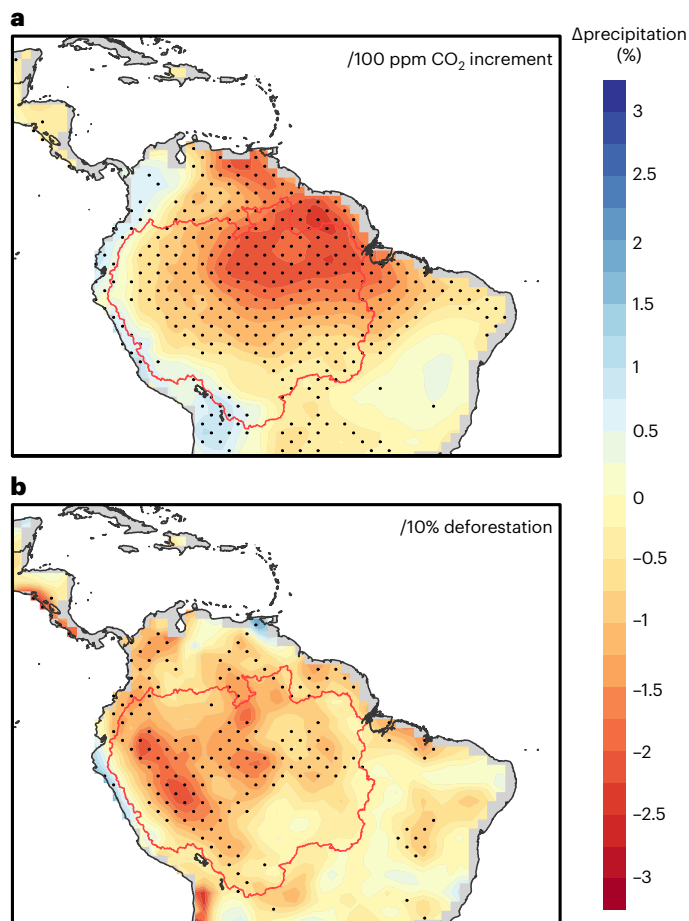


Fig. 2 | Spatial distribution of the mean annual precipitation response to forcing from CO₂ physiology and deforestation. a, b, Precipitation response to 100 ppm CO₂ increase (a) and 10% loss in forest fraction (b). The precipitation changes were computed in per cent from each model and then averaged across CMIP6 models. Linear regressions were performed for the precipitation at each pixel against atmospheric CO₂ concentrations (a) and basin-scale average in forest cover loss (b) from their 140 year and 50 year simulations of the C4MIP and LUMIP experiments, respectively (Methods). The dotted areas indicate places with model agreement, with at least six out of eight models agreeing on the sign of the precipitation response.

SSP scenarios have different pathways of future atmospheric CO₂ concentration and land use, depending on different assumptions about the strength of international cooperation, technology and economic development¹⁴. SSP1-2.6 has been described as the most sustainable future with global temperature stabilizing below 2 °C of warming by 2081–2100 (ref. 44). In this scenario, atmospheric CO₂ increases slowly, reaching a maximum of 474 ppm in 2063, and then declining to a mean level of 456 ppm by 2081–2100. By contrast, atmospheric CO₂ concentrations under the other three scenarios keep rising throughout the twenty-first century, reaching 597 ppm for SSP2-4.5, 792 ppm for SSP3-7.0 and 1,005 ppm for SSP5-8.5. The CO₂ increments for these SSPs, relative to the background level in 1850 for the pre-industrial control, are summarized in Fig. 3.

Although SSP5-8.5 has the highest atmospheric CO₂ increase, its assumptions regarding global energy development are not closely coupled to land use change, and therefore the deforestation fraction in the Amazon basin remains nearly constant at 6.4% from 2021–2040 through 2081–2100. This projection is similar to the 6.1% deforestation fraction for SSP1-2.6. For SSP2-4.5, Amazonian deforestation first increases to 8.3% during 2041–2060 and then decreases to 5.2% during 2081–2100 as a consequence of forest recovery (Fig. 3b). The greatest

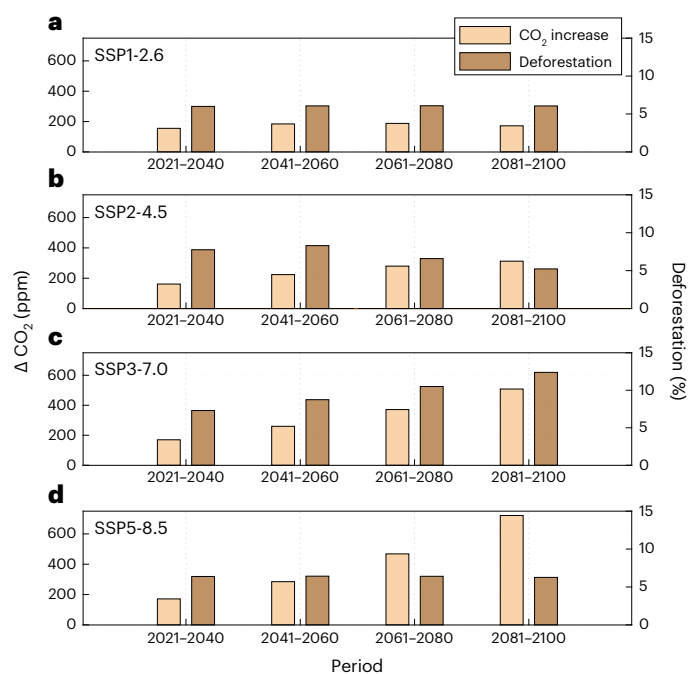


Fig. 3 | Changes in CO₂ concentrations and deforestation fraction of the Amazon basin in SSPs. a–d, Both CO₂ increase (light brown) and loss in forest fraction of the Amazon basin (red brown) were computed as the difference between future projections and the pre-industrial levels for SSP1-2.6 (a), SSP2-4.5 (b), SSP3-7.0 (c) and SSP5-8.5 (d). Future projections were derived from CMIP6 ScenarioMIP for different future SSPs.

Amazonian forest cover loss occurs under SSP3-7.0 where deforestation increases to 12.4% by 2081–2100 (Fig. 3c).

Precipitation decreases by 4.8% (−0.26 mm per day) for SSP1-2.6 by 2081–2020 relative to the pre-industrial mean level in 1850 (5.5 mm per day). For this scenario, we find that the sum of contributions from CO₂ physiology and deforestation account for 46% (−0.12 mm per day) of future precipitation decline over the Amazon basin (Fig. 4a). Similarly, of the 13.2% decline (−0.72 mm per day) in Amazonia precipitation occurring by 2100 for SSP3-7.0, 44% of this decrease (−0.32 mm per day) can be attributed to the combined effect of CO₂ physiology and deforestation. Across all the different future scenarios and time intervals shown in Fig. 4, the combined contributions of CO₂ physiology and deforestation to Amazonian precipitation change vary between 34% and 56% (Fig. 4). For surface RH, a key driver of fire risk^{45,46}, the impact of CO₂ physiology and deforestation is even greater in magnitude, accounting for 48% of the RH decline for SSP3-7.0 and 52% for SSP5-8.5 (Supplementary Fig. 4). These findings highlight the importance of decreases in surface evapotranspiration due to both CO₂ physiology and deforestation (Supplementary Fig. 5a,b) as key model drivers influencing the future hydroclimate of the Amazon basin (Fig. 5).

By contrast, for surface air temperature, the contribution from the two drivers to warming is relatively small, primarily because of the stronger regional and global temperature response to radiative forcing from greenhouse gases. For example, for SSP3-7.0 about 11% of future Amazonian warming can be attributed to forcing from CO₂ physiology and deforestation by the end of the century (Fig. 5 and Supplementary Fig. 6).

Solely considering contributions from the response of physiology to rising CO₂, precipitation declines ranged between 33% for SSP1-2.6 and 46% for SSP5-8.5 (Fig. 4a,d). Deforestation contributions to precipitation declines varied between 4% for SSP5-8.5 and 13% for SSP1-2.6. CO₂ physiology also had a much larger impact than deforestation for RH and temperature changes within the different SSP simulations.

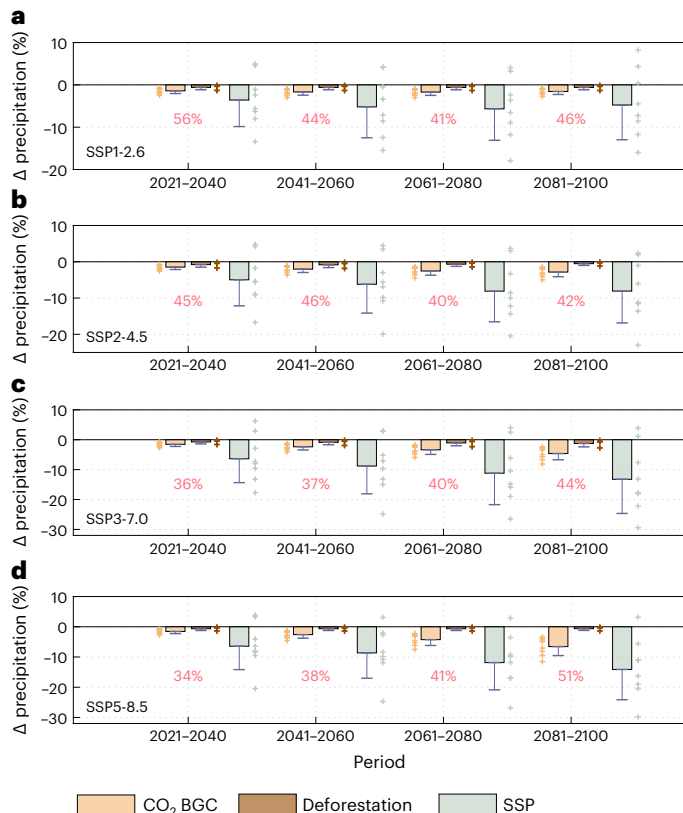


Fig. 4 | Climate contributions of CO₂ physiology and deforestation to future changes in precipitation over the Amazon basin. a–d. Future changes in Amazonian precipitation (%) due to CO₂ physiological effects (light brown) and deforestation (red brown) were computed from the precipitation response from these two drivers (Methods). Light grey indicates the future Amazonian precipitation changes under the four SSPs during different periods: SSP1-2.6 (a), SSP2-4.5 (b), SSP3-7.0 (c) and SSP5-8.5 (d). Red numbers indicate the percentage of total precipitation changes for each period and SSP attributed to CO₂ physiology and deforestation. Each error bar indicates one standard deviation added to the mean values across the CMIP6 models with available output ($n = 8$ for CO₂ physiology and SSP simulation, $n = 6$ for deforestation). Data point for each model has been shown along with the bar indicated by a plus sign. Relative precipitation changes in per cent can be converted to absolute changes in mm per day by multiplying by a multi-model mean annual precipitation of 5.5 mm per day for the pre-industrial period.

Discussion

CO₂ physiology and deforestation are found to account for over 40% of the declines in both precipitation and surface RH in the Amazon basin by the end of the twenty-first century (Fig. 4 and Supplementary Fig. 4). These results indicate that a considerable amount of future Amazonian precipitation and meteorological drought^{7–12} can be attributed to drivers other than the radiative effects of greenhouse gases and aerosols. The important role of climate forcing from the land surface could enable a relatively fast (and positive) hydroclimate response in the Amazon basin if climate policies are enacted that allow for reforestation or a decline in atmospheric CO₂ levels. This contrasts with the considerably slower (multi-decadal) response time of climate to radiative forcing from greenhouse gases as a consequence of long-term adjustments in ocean heating⁴⁷. The estimated contributions of deforestation to future precipitation at the basin scale vary between 4% and 13% across the different SSPs. These estimates also serve as a range for the potential co-benefits in hydroclimate that could be achieved by preventing further deforestation, complementing carbon and ecological co-benefits reported in previous work⁴⁸.

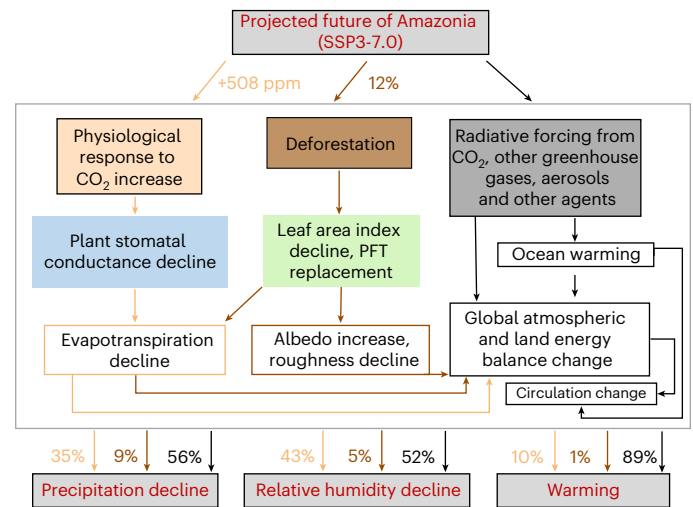


Fig. 5 | Conceptual diagram of the mechanisms by which CO₂ physiology and deforestation influence climate change in the Amazon basin. Taking the SSP3-7.0 as an example, the contributions of CO₂ physiology and deforestation to Amazonian climate change by the end of the twenty-first century (2081–2100) were quantified using the CMIP6 idealized experiments described in Methods. More information about evapotranspiration, albedo and leaf area index model responses, which have a key role in regulating the integrated climate response, can be found in Supplementary Fig. 5. PFT, plant functional type. Additional analysis of the underlying mechanisms can be found in previous work by Swann et al.²⁴, Zhou et al.²⁷ and Boysen et al.²⁸.

As a consequence of land–atmosphere interactions, past work has identified a loss of 40% of forest within the Amazon basin as a ‘tipping point’, beyond which hydroclimate changes would threaten the viability of remaining forests³¹. Our analysis also points to the negative consequences of deforestation for precipitation but additionally suggests that, at least for widely analysed SSPs, threats to the future hydroclimate of the Amazon basin are even larger from the radiative effects of greenhouse gases and aerosols and from direct ecosystem responses to rising levels of atmospheric CO₂.

The substantial contributions of CO₂ physiology to future Amazonian precipitation change in CMIP6 SSP simulations highlight the importance of improving our knowledge of land–atmosphere interactions and their response to climate change, atmospheric CO₂ and deforestation within the Amazon basin⁴⁹. For rising CO₂, key drivers of the land surface response include changes in evapotranspiration, albedo, and leaf area index shown in Supplementary Fig. 5. To reduce model uncertainties, additional observations and model simulation are needed to understand subsequent changes in boundary layer, deep convection and regional circulation. While CMIP models provided a coherent and robust response to CO₂ forcing associated with plant physiology, the magnitude of this response remains highly uncertain mainly because there are relatively few ecosystem-level observations from tropical forests available for model testing. This highlights the importance of new, sustained stomatal conductance and evapotranspiration measurements at different CO₂ levels, such as those planned as a part of the Amazon FACE experiment⁵⁰. Additionally, acclimation of stomatal conductance responses to long-term increasing levels of atmospheric CO₂ remains a key unresolved issue in this respect⁵¹.

Other key process-based uncertainties include the representation of land–atmosphere coupling and atmospheric convection that influence the precipitation recycling ratio in the Amazon basin⁵², and the ability of the models to capture the influence of changing ocean dynamics on future atmospheric circulation (and precipitation). For example, a recent study reported there is a systematic bias in CMIP6 models in capturing the cooling signal over the eastern equatorial

Pacific in the past four decades⁵³. Such a cooling pattern resembles a La-Niña-like condition that could increase the precipitation in the Amazon basin through changes in local Walker circulation⁵⁴. Some of the model-to-model differences in the magnitude of the SSP precipitation response (shown with the error bars in Fig. 4; Supplementary Table 3) can probably be traced back to the ocean response to radiative forcing from greenhouse gases and aerosols^{55,56}, which also needs further exploration in future work.

For deforestation, paths for reducing uncertainty in coupled model estimates of the Amazonian climate response include more extensive comparison of models with observations and refinement of the LUMIP protocol for CMIP7. In this study, we report that the local biophysical temperature effects range from -0.19°C to 0.15°C in response to 10% deforestation in the Amazon basin (Supplementary Table 2). Although the multi-model mean warming response is consistent with past work⁴¹, variability in the magnitude of the response across the different CMIP models is large and stems from at least three possible sources. First, there is a difference in the level of calibration and validation efforts from each modelling group to improve the biophysical temperature effects of deforestation. For example, the land model component of CESM2, the Community Land Model, has been improved through parameter optimization⁵⁷ and benchmarking with satellite observations⁵⁸. Second, there are still a limited number of observations in the Amazon basin to help with the model calibration. For instance, a recent comparison of biogeochemical and biophysical climate effects of deforestation⁵⁹, which includes observational datasets from Bright et al.⁶⁰ and Duveiller et al.⁶¹, is still limited by a paucity of paired forested and non-forested eddy-covariance sites and relatively sparse satellite data coverage due to frequently cloudy conditions. Third, the CMIP6 LUMIP deforestation protocol is global in scope²⁸. In designing the future LUMIP protocol for CMIP7, consideration of a tropical-only experiment with an increased number of ensemble members may provide a stronger basis for robustly characterizing regional climate responses. Further analysis of drought and fire metrics in LUMIP simulations, including soil moisture and burned area, is also needed to understand better the processes of regional-scale dynamic vegetation feedbacks to Amazonia hydroclimate from changes in forest cover.

By recognizing the relatively fast adjustment time and linear relationship between land surface forcing and Amazonian climate response, we developed a first attempt to separate CO₂ physiology and deforestation contributions to climate change in CMIP6 SSP simulations. While the assumption of linearity and independence of the two forcing agents simplified our analysis, it is important to recognize potential interactions and feedback between these two drivers and target these interactions in future work. Further deforestation, for example, may weaken the regional climate response to rising CO₂ as forests are replaced with pastures and grasslands that have a lower surface roughness and canopy fraction for transpiration. Across the SSPs, the deforestation fraction is generally small, as predicted in the SSPs by the end of the twenty-first century and ranges from 5.2% in SSP2-4.5 to 12.4% in SSP3-7.0. To estimate the potential magnitude of some of these interactions, we performed a back-of-the-envelope calculation. Specifically, for the SSP3-7.0 scenario, we reduced the CO₂ physiological contribution by 12% to reflect the concurrent loss of total forest cover. With this simple assumption, which is probably an upper bound due to the largest deforestation fraction of 12%, the precipitation decline attributed to CO₂ physiology decreases from 35% to 31%. Some additional non-linearities are likely to be introduced from interactions between the radiative effects of greenhouse gases and the land surface forcing mechanisms explored here. Supplementary Fig. 7, for example, shows that the CO₂ physiology effect on precipitation is largely independent of the deforestation effect but has a weak relationship with precipitation response to the CO₂ radiative effect. These illustrative calculations and analysis suggest that interactions may slightly reduce our estimated magnitude of precipitation effects but are unlikely to

change our study's main findings qualitatively. This also highlights the need to explore feedback between forcing agents in future work. One effective way to accomplish this in CMIP7 would be to add a CO₂ physiology simulation (for example, a BGC simulation) and a land use simulation to the DAMIP⁶² for historical and one to two SSPs to 2100.

In this study, we provide an attribution analysis of Amazonian climate change in widely used SSP simulations by isolating contributions from the plant physiological response to rising CO₂ and deforestation. We accomplish this by combining information from two different idealized experiments from CMIP6. From the idealized (biogeochemically coupled) CO₂ experiment from C4MIP and the idealized deforestation experiment from LUMIP, we identify that the climate change response to feedbacks from changes in the land surface are rapid and mostly linear across the basin and across the dynamic range of CO₂ concentration and land cover change captured by the SSPs. The combined effects from the two drivers account for more than 40% of future basin-wide precipitation and surface RH declines, but less than 11% of warming over the Amazon basin by the end of the twenty-first century. This implies a substantial contribution from CO₂ physiology and deforestation to increasing risk of future meteorological drought and wildfire. Our findings provide insight about the sources of uncertainty of climate model projections and may help with identifying the full scope of climate benefits associated with forest conservation policies in the Amazon basin.

Methods

We isolated the climate change response in the Amazon basin to CO₂ physiology and deforestation using output from two idealized CMIP6 experiments. From C4MIP⁴² we analysed the idealized 140 year simulations (1pctCO2-bgc) in which CO₂ concentrations increase by 1% per year, but the CO₂ increases are not radiatively active (that is, all models' radiation code uses a constant atmospheric CO₂ concentration that was held constant at the pre-industrial level). The 1pctCO2-bgc experiment from C4MIP allows for the isolation of the climate response resulting from plant physiological responses to rising CO₂. From LUMIP⁴³ we analysed a global idealized deforestation experiment (deforest-glob). The LUMIP deforest-glob simulation has an 80 year duration with a total forest area of 20 million km² linearly removed from each model's top 30% of forest grid cells across the globe during the first 50 years. This results in about a 0.9% per year decline in tree cover fraction across the Amazon basin as a whole (that is, the deforestation was mostly spatially homogeneous in the simulations). Since there are only deforestation effects in this experiment, changes in Amazonia climate can be attributed solely to this driver.

In a second step, we identified the contribution of plant physiology responses to rising CO₂ and deforestation to Amazonian climate change within CMIP6 future scenario experiments (ScenarioMIP)¹³. We focused on CMIP6 simulations for four widely used SSPs¹⁴. These SSP simulations have different radiative forcing levels by 2100. They are: SSP1-2.6, SSP2-4.5, SSP3-7.0 and SSP5-8.5. The number behind each future scenario (for example, 8.5 for SSP5-8.5) indicates the radiative forcing level (unit: W/m²) that occurs in the scenario by 2100. To quantify the relative change in Amazonian climate in the future, we also include the pre-industrial control (piControl) experiment of CMIP6 that uses fixed radiative forcing identical to the level during 1850. The year of 1850 is also the reference year in our study.

Monthly air temperature (tas), precipitation (pr), surface RH (hurs), and tree cover (treeFrac) during the historical and future periods from the above CMIP6 experiments were downloaded from the archive of Earth System Grid Federation. Before analysis, all variables were remapped to a 1-degree grid using the bilinear interpolation method from Climate Data Operator⁶³. Because not all CMIP6 modelling centres participated in all four experiments as described above, we chose to use eight models that have the maximum availability of these variables (Supplementary Table 1). They include BCC-CSM2-MR (Wu et al.⁶⁴),

CanESM5 (Swart et al.⁶⁵), CESM2 (Danabasoglu et al.⁶⁶), CNRM-ESM2-1 (Seferian et al.⁶⁷), IPSL-CM6A-LR (Boucher et al.⁶⁸), GISS-E2-1-G (Kelley et al.⁶⁹), UKESM1-0-LL (Sellar et al.⁷⁰) and MPI-ESM1-2-LR (Mauritsen et al.⁷¹). To obtain the most robust climate response to CO₂ physiology and deforestation as possible, climate variables were averaged for each model across ensemble members based on their availability in both the C4MIP and LUMIP experiments (Supplementary Table 1). The ensemble mean approach helps improve the signal-to-noise ratio of the climate response to CO₂ physiology or deforestation in the Amazon basin, considering the different influences from interannual variability from each model. Yet, it also relies on the mechanism coherence and traceability across these models. For future SSP scenarios, atmospheric CO₂ concentrations during the twenty-first century were obtained from the input datasets for Model Intercomparison Projects (input4MIPs), and their land use including the fraction of forest in the Amazon basin was obtained from the Land Use Harmonization dataset version 2 (LUHv2f, ref. 72).

To isolate the precipitation response to either plant physiological response to increasing CO₂ or deforestation within the eight CMIP6 models, the relative precipitation changes in per cent were computed relative to the pre-industrial average for each model in each experiment before determining the average across models. We used simple linear regression equations to describe the response of precipitation, surface RH and surface air temperature to CO₂ concentration and forest cover percentage.

$$y = \alpha + \beta x$$

where y indicates the climate variables such as precipitation, surface RH or surface air temperature, and x indicates either CO₂ concentration change or deforestation fraction over the Amazon basin. β and α are the slope and y -intercept as estimated from the above equation, respectively. As shown in Fig. 1, the estimated β at the basin scale was used as the climate sensitivity to either CO₂ concentrations in C4MIP 1pctCO₂-bgc or deforestation fraction in LUMIP deforest-glob. The y -axis intercept value in Fig. 1 may not be identical to 100% for precipitation and to 0 for surface air temperature, probably from the influence of the internal variability. We chose not to force the regressions through a specified y -axis intercept to avoid overestimating contributions from CO₂ physiology and deforestation in our attribution analysis. To assess the spatial pattern of the Amazonian climate response, we also performed the linear regression analysis for each model pixel.

To estimate the contribution of plant physiological response to CO₂ to future climate change in the Amazon basin, we first computed the changes in the atmospheric CO₂ concentration from the pre-industrial era (that is, 1850) to different future periods (that is, 2021–2040, 2041–2060, 2061–2080 and 2081–2100). We then multiplied this CO₂ change with the slope derived from the linear regression describing the response of each climate variable to atmospheric CO₂ concentration from the C4MIP 1pctCO₂-bgc simulations (left column in Fig. 1). In the 1pctCO₂-bgc simulations, land cover was held constant throughout the simulations at 1850 levels. Similarly, the deforestation contributions were computed as the product of the basin-scale average deforestation fraction from each of the future SSPs scenarios relative to 1850 forest cover, and the slope derived from the linear regression describing the response of each climate variable to Amazonian deforestation fraction from the LUMIP deforest-glob simulations (right column in Fig. 1). In the LUMIP simulation atmospheric CO₂ concentration was held constant at 1850 levels⁴³. The regression approach was applied for the purpose of deriving the sensitivity of the climate response to CO₂ concentration or deforestation fraction, respectively, using the different C4MIP and LUMIP simulations. The contribution by either CO₂ physiology or deforestation was estimated for the whole Amazon basin, as shown in Fig. 4 and Supplementary Figs. 4 and 6.

We assumed that the climate response to CO₂ physiological forcing and deforestation could be isolated from the CMIP6 simulations because climate responses to land surface forcing, including adjustments in boundary layer height and convection from changes in surface evapotranspiration, are known to be relatively fast, occurring over timescales of days to weeks³⁵. Raw data underlying each figure can be found in ref. 73.

Reporting summary

Further information on research design is available in the Nature Portfolio Reporting Summary linked to this article.

Data availability

All CMIP6 simulations used in this study are publicly available at <https://esgf-node.llnl.gov/projects/cmip6/>. Atmospheric CO₂ concentrations for future SSP scenarios were downloaded from <https://esgf-node.llnl.gov/projects/input4mips/>. Future land use datasets LUHv2f were downloaded from <https://luh.umd.edu/data.shtml>. Data supporting each major figure can be accessed from ref. 73. Raw data underlying figures from Figs. 1–4 are available at <https://doi.org/10.6084/m9.figshare.23826222>.

Code availability

All computer codes used in this study are available via GitHub at https://github.com/YueLi92/Contributions_CO2Phys_Def_SSP.

References

- Malhi, Y. et al. Exploring the likelihood and mechanism of a climate-change-induced dieback of the Amazon rainforest. *Proc. Natl Acad. Sci. USA* **106**, 20610–20615 (2009).
- Phillips, O. L. et al. Drought sensitivity of the Amazon rainforest. *Science* **323**, 1344–1347 (2009).
- Brando, P. M. et al. Abrupt increases in Amazonian tree mortality due to drought–fire interactions. *Proc. Natl Acad. Sci. USA* **111**, 6347–6352 (2014).
- Aragão, L. E. et al. 21st century drought-related fires counteract the decline of Amazon deforestation carbon emissions. *Nat. Commun.* **9**, 1–12 (2018).
- Orlowsky, B. & Seneviratne, S. I. Elusive drought: uncertainty in observed trends and short-and long-term CMIP5 projections. *Hydrol. Earth Syst. Sci.* **17**, 1765–1781 (2013).
- Mankin, J. S., Seager, R., Smerdon, J. E., Cook, B. I. & Williams, A. P. Mid-latitude freshwater availability reduced by projected vegetation responses to climate change. *Nat. Geosci.* **12**, 983–988 (2019).
- Cook, B. I. et al. Twenty-first century drought projections in the CMIP6 forcing scenarios. *Earth Future* **8**, e2019EF001461 (2020).
- Parsons, L. A. Implications of CMIP6 projected drying trends for 21st century Amazonian drought risk. *Earth Future* **8**, e2020EF001608 (2020).
- Ukkola, A. M., De Kauwe, M. G., Roderick, M. L., Abramowitz, G. & Pitman, A. J. Robust future changes in meteorological drought in CMIP6 projections despite uncertainty in precipitation. *Geophys. Res. Lett.* **47**, e2020GL087820 (2020).
- Fan, X., Miao, C., Duan, Q., Shen, C. & Wu, Y. Future climate change hotspots under different 21st century warming scenarios. *Earth Future* **9**, e2021EF002027 (2021).
- Li, H. et al. Drylands face potential threat of robust drought in the CMIP6 SSPs scenarios. *Environ. Res. Lett.* **16**, 114004 (2021).
- Zhao, T. & Dai, A. CMIP6 model-projected hydroclimatic and drought changes and their causes in the twenty-first century. *J. Clim.* **35**, 897–921 (2022).
- O'Neill, B. C. et al. The scenario model intercomparison project (ScenarioMIP) for CMIP6. *Geosci. Model Dev.* **9**, 3461–3482 (2016).

14. Riahi, K. et al. The shared socioeconomic pathways and their energy, land use, and greenhouse gas emissions implications: an overview. *Glob. Environ. Change* **42**, 153–168 (2017).
15. Boit, A. et al. Large-scale impact of climate change vs. land-use change on future biome shifts in Latin America. *Glob. Chang. Biol.* **22**, 3689–3701 (2016).
16. Koch, A. & Kaplan, J. O. Tropical forest restoration under future climate change. *Nat. Clim. Change* **12**, 279–283 (2022).
17. Munia, H. A. et al. Future transboundary water stress and its drivers under climate change: a global study. *Earth Future* **8**, e2019EF001321 (2020).
18. Park, C. Y. et al. How Will deforestation and vegetation degradation affect global fire activity? *Earth Future* **9**, e2020EF001786 (2021).
19. Silva, M. V. M. D. et al. Naturalized streamflows and Affluent Natural Energy projections for the Brazilian hydropower sector for the SSP2-4.5 and SSP5-8.5 scenarios of the CMIP6. *J. Water Clim. Chang.* **13**, 315–336 (2021).
20. Hall, A. & Qu, X. Using the current seasonal cycle to constrain snow albedo feedback in future climate change. *Geophys. Res. Lett.* **33**, L03502 (2006).
21. Chen, Y., Langenbrunner, B. & Randerson, J. T. Future drying in central america and northern south america linked with atlantic meridional overturning circulation. *Geophys. Res. Lett.* **45**, 9226–9235 (2018).
22. Duffy, P. B., Brando, P., Asner, G. P. & Field, C. B. Projections of future meteorological drought and wet periods in the Amazon. *Proc. Natl Acad. Sci. USA* **112**, 3172–3177 (2015).
23. Boisier, J. P., Ciais, P., Ducharne, A. & Guimberteau, M. Projected strengthening of Amazonian dry season by constrained climate model simulations. *Nat. Clim. Change* **5**, 656–660 (2015).
24. Swann, A. L., Hoffman, F. M., Koven, C. D. & Randerson, J. T. Plant responses to increasing CO₂ reduce estimates of climate impacts on drought severity. *Proc. Natl Acad. Sci. USA* **113**, 10019–10024 (2016).
25. Kooperman, G. J. et al. Forest response to rising CO₂ drives zonally asymmetric rainfall change over tropical land. *Nat. Clim. Change* **8**, 434–440 (2018).
26. Richardson, T. B. et al. Carbon dioxide physiological forcing dominates projected eastern Amazonian drying. *Geophys. Res. Lett.* **45**, 2815–2825 (2018).
27. Zhou, S., Yu, B., Lintner, B., Findell, K. L. & Zhang, Y. Projected increase in global runoff dominated by land surface changes. *Nat. Clim. Change* **13**, 442–449 (2023).
28. Boysen, L. R. et al. Global climate response to idealized deforestation in CMIP6 models. *Biogeosciences* **17**, 5615–5638 (2020).
29. Luo, X. et al. The biophysical impacts of deforestation on precipitation: results from the CMIP6 model intercomparison. *J. Clim.* **35**, 3293–3311 (2022).
30. Lehner, F. et al. Partitioning climate projection uncertainty with multiple large ensembles and CMIP5/6. *Earth Syst. Dynam.* **11**, 491–508 (2020).
31. Nobre, C. A. et al. Land-use and climate change risks in the Amazon and the need of a novel sustainable development paradigm. *Proc. Natl Acad. Sci. USA* **113**, 10759–10768 (2016).
32. Marengo, J. A. et al. Changes in climate and land use over the Amazon region: current and future variability and trends. *Front. Earth Sci.* **6**, 228 (2018).
33. Held, I. M. & Soden, B. J. Robust responses of the hydrological cycle to global warming. *J. Clim.* **19**, 5686–5699 (2006).
34. He, J. & Soden, B. J. A re-examination of the projected subtropical precipitation decline. *Nat. Clim. Change* **7**, 53–57 (2017).
35. Langenbrunner, B., Pritchard, M. S., Kooperman, G. J. & Randerson, J. T. Why does Amazon precipitation decrease when tropical forests respond to increasing CO₂? *Earth Future* **7**, 450–468 (2019).
36. Khanna, J., Medvigy, D., Fisch, G. & de Araujo Tiburtino Neves, T. T. Regional hydroclimatic variability due to contemporary deforestation in southern Amazonia and associated boundary layer characteristics. *J. Geophys. Res. Atmos.* **123**, 3993–4014 (2018).
37. Maeda, E. E. et al. Large-scale commodity agriculture exacerbates the climatic impacts of Amazonian deforestation. *Proc. Natl Acad. Sci. USA* **118**, e2023787118 (2021).
38. Leite-Filho, A. T., Soares-Filho, B. S., Davis, J. L., Abrahão, G. M. & Börner, J. Deforestation reduces rainfall and agricultural revenues in the Brazilian Amazon. *Nat. Commun.* **12**, 1–7 (2021).
39. Spracklen, D. V. & Garcia-Carreras, L. J. G. R. L. The impact of Amazonian deforestation on Amazon basin rainfall. *Geophys. Res. Lett.* **42**, 9546–9552 (2015).
40. Sampaio, G. et al. CO₂ physiological effect can cause rainfall decrease as strong as large-scale deforestation in the Amazon. *Biogeosciences* **18**, 2511–2525 (2021).
41. Lawrence, D. & VandeCar, K. Effects of tropical deforestation on climate and agriculture. *Nat. Clim. Change* **5**, 27–36 (2015).
42. Jones, C. D. et al. C4MIP—the coupled climate–carbon cycle model intercomparison project: experimental protocol for CMIP6. *Geosci. Model Dev.* **9**, 2853–2880 (2016).
43. Lawrence, D. M. et al. The Land Use Model Intercomparison Project (LUMIP) contribution to CMIP6: rationale and experimental design. *Geosci. Model Dev.* **9**, 2973–2998 (2016).
44. IPCC Summary for Policymakers. In *Climate Change 2021: The Physical Science Basis. Contribution of Working Group I to the Sixth Assessment Report of the Intergovernmental Panel on Climate Change* 3–32 (eds Masson-Delmotte, V. et al.) (Cambridge Univ. Press, 2021).
45. Balch, J. K. et al. Warming weakens the night-time barrier to global fire. *Nature* **602**, 442–448 (2022).
46. Jain, P., Castellanos-Acuna, D., Coogan, S. C. P., Abatzoglou, J. T. & Flannigan, M. D. Observed increases in extreme fire weather driven by atmospheric humidity and temperature. *Nat. Clim. Change* **12**, 63–70 (2022).
47. Cheng, L. et al. Past and future ocean warming. *Nat. Rev. Earth Environ.* **3**, 776–794 (2022).
48. Stickler, C. M. et al. The potential ecological costs and cobenefits of REDD: a critical review and case study from the Amazon region. *Glob. Change Biol.* **15**, 2803–2824 (2009).
49. Zemp, D. C. et al. Self-amplified Amazon forest loss due to vegetation-atmosphere feedbacks. *Nat. Commun.* **8**, 1–10 (2017).
50. Norby, R. J. et al. Model–data synthesis for the next generation of forest free-air CO₂ enrichment (FACE) experiments. *New Phytol.* **209**, 17–28 (2016).
51. Medlyn, B. E. et al. Stomatal conductance of forest species after long-term exposure to elevated CO₂ concentration: a synthesis. *New Phytol.* **149**, 247–264 (2008).
52. Baker, J. C. A. & Spracklen, D. V. Divergent representation of precipitation recycling in the Amazon and the Congo in CMIP6 models. *Geophys. Res. Lett.* **49**, E2021GL095136 (2022).
53. Wills, R. C. J., Dong, Y., Proistosescu, C., Armour, K. C. & Battisti, D. S. Systematic climate model biases in the large-scale patterns of recent sea-surface temperature and sea-level pressure change. *Geophys. Res. Lett.* **49**, e2022GL100011 (2022).
54. Barichivich, J. et al. Recent intensification of Amazon flooding extremes driven by strengthened Walker circulation. *Sci. Adv.* **4**, eaat8785 (2018).
55. Weijer, W., Cheng, W., Garuba, O. A., Hu, A. & Nadiga, B. T. CMIP6 models predict significant 21st century decline of the Atlantic Meridional Overturning Circulation. *Geophys. Res. Lett.* **47**, e2019GL086075 (2020).
56. Ciemer, C., Winkelmann, R., Kurths, J. & Boers, N. Impact of an AMOC weakening on the stability of the southern Amazon rainforest. *Eur. Phys. J. Spec. Top.* **230**, 3065–3073 (2021).

57. Cai, X. et al. Improving representation of deforestation effects on evapotranspiration in the E3SM land model. *J. Adv. Model. Earth Syst.* **11**, 2412–2427 (2019).
58. Chen, L. & Dirmeyer, P. A. Reconciling the disagreement between observed and simulated temperature responses to deforestation. *Nat. Commun.* **11**, 1–10 (2020).
59. Windisch, M. G., Davin, E. L. & Seneviratne, S. I. Prioritizing forestation based on biogeochemical and local biogeophysical impacts. *Nat. Clim. Change* **11**, 867–871 (2021).
60. Bright, R. M. et al. Local temperature response to land cover and management change driven by non-radiative processes. *Nat. Clim. Change* **7**, 296–302 (2017).
61. Duveiller, G., Hooker, J. & Cescatti, A. The mark of vegetation change on Earth's surface energy balance. *Nat. Commun.* **9**, 1–12 (2018).
62. Gillet, N. P. et al. The Detection and Attribution Model Intercomparison Project (DAMIP v1.0) contribution to CMIP6. *Geosci. Model Dev.* **9**, 3685–3697 (2016).
63. Schulzweida, U. Climate data operators (CDO) user guide (Version 1.9.8). Zenodo <https://doi.org/10.5281/zenodo.3539275> (2019).
64. Wu, T. et al. The Beijing Climate Center climate system model (BCC-CSM): the main progress from CMIP5 to CMIP6. *Geosci. Model Dev.* **12**, 1573–1600 (2019).
65. Swart, N. C. et al. The Canadian Earth System Model version 5 (CanESM5. 0.3). *Geosci. Model Dev.* **12**, 4823–4873 (2019).
66. Danabasoglu, G. et al. The Community Earth System Model version 2 (CESM2). *J. Adv. Model Earth Syst.* **12**, e2019MS001916 (2020).
67. Séférian, R. et al. Evaluation of CNRM Earth System Model, CNRM-ESM2-1: role of Earth system processes in present-day and future climate. *J. Adv. Model Earth Syst.* **11**, 4182–4227 (2019).
68. Boucher, O. et al. Presentation and evaluation of the IPSL-CM6A-LR climate model. *J. Adv. Model Earth Syst.* **12**, 1–52 (2020).
69. Kelley, M. et al. GISS-E2. 1: configurations and climatology. *J. Adv. Model Earth Syst.* **12**, e2019MS002025 (2020).
70. Sellar, A. A. et al. Implementation of UK Earth system models for CMIP6. *J. Adv. Model Earth Syst.* **12**, e2019MS001946 (2020).
71. Mauritsen, T. et al. Developments in the MPI-M Earth System Model version 1.2 (MPI-ESM1. 2) and its response to increasing CO₂. *J. Adv. Model Earth Syst.* **11**, 998–1038 (2019).
72. Hurtt, G. C. et al. Harmonization of global land use change and management for the period 850–2100 (LUH2) for CMIP6. *Geosci. Model Dev.* **13**, 5425–5464 (2020).
73. Li, Y. et al. Raw data underlying figures from Fig. 1 to Fig. 4, Figshare, <https://doi.org/10.6084/m9.figshare.23826222> (2023).

Acknowledgements

Y.L. and J.T.R. acknowledge support from the US Department of Energy (DOE) Office of Science, Biological and Environmental Research (BER), Earth and Environmental Systems Modeling programme to study dust and fire (DE-SC0021302) and the RUBISCO Scientific Focus Area. J.T.R. and D.C.M. received funding support from NASA's SERVIR and MAP research programmes. A.L.S.S. recognizes funding support from DOE BER Regional and Global Model Analysis programme (DE-SC0021209). The funders had no role in study design, data collection and analysis, the decision to publish, or manuscript preparation.

Author contributions

Y.L. and J.T.R. designed the research; Y.L. performed data analysis and figure illustrations; Y.L. and J.T.R. drafted the manuscript, with discussions and contributions from J.C.A.B., P.M.B., F.M.H., D.M.L., D.C.M., A.L.S.S. and M.R.U.; all authors reviewed and revised the manuscript.

Competing interests

The authors declare no competing interests.

Additional information

Supplementary information The online version contains supplementary material available at <https://doi.org/10.1038/s44221-023-00128-y>.

Correspondence and requests for materials should be addressed to Yue Li.

Peer review information *Nature Water* thanks David Lapola, Markus Reichstein, Corey Lesk and Alexander Winkler for their contribution to the peer review of this work.

Reprints and permissions information is available at www.nature.com/reprints.

Publisher's note Springer Nature remains neutral with regard to jurisdictional claims in published maps and institutional affiliations.

Springer Nature or its licensor (e.g. a society or other partner) holds exclusive rights to this article under a publishing agreement with the author(s) or other rightsholder(s); author self-archiving of the accepted manuscript version of this article is solely governed by the terms of such publishing agreement and applicable law.

© The Author(s), under exclusive licence to Springer Nature Limited 2023

Corresponding author(s): Yue Li

Last updated by author(s): Nov 22, 2022

Reporting Summary

Nature Portfolio wishes to improve the reproducibility of the work that we publish. This form provides structure for consistency and transparency in reporting. For further information on Nature Portfolio policies, see our [Editorial Policies](#) and the [Editorial Policy Checklist](#).

Statistics

For all statistical analyses, confirm that the following items are present in the figure legend, table legend, main text, or Methods section.

n/a Confirmed

- | | | |
|-------------------------------------|-------------------------------------|--|
| <input type="checkbox"/> | <input checked="" type="checkbox"/> | The exact sample size (n) for each experimental group/condition, given as a discrete number and unit of measurement |
| <input checked="" type="checkbox"/> | <input type="checkbox"/> | A statement on whether measurements were taken from distinct samples or whether the same sample was measured repeatedly |
| <input checked="" type="checkbox"/> | <input type="checkbox"/> | The statistical test(s) used AND whether they are one- or two-sided
<i>Only common tests should be described solely by name; describe more complex techniques in the Methods section.</i> |
| <input checked="" type="checkbox"/> | <input type="checkbox"/> | A description of all covariates tested |
| <input checked="" type="checkbox"/> | <input type="checkbox"/> | A description of any assumptions or corrections, such as tests of normality and adjustment for multiple comparisons |
| <input type="checkbox"/> | <input checked="" type="checkbox"/> | A full description of the statistical parameters including central tendency (e.g. means) or other basic estimates (e.g. regression coefficient) AND variation (e.g. standard deviation) or associated estimates of uncertainty (e.g. confidence intervals) |
| <input checked="" type="checkbox"/> | <input type="checkbox"/> | For null hypothesis testing, the test statistic (e.g. F , t , r) with confidence intervals, effect sizes, degrees of freedom and P value noted
<i>Give P values as exact values whenever suitable.</i> |
| <input checked="" type="checkbox"/> | <input type="checkbox"/> | For Bayesian analysis, information on the choice of priors and Markov chain Monte Carlo settings |
| <input checked="" type="checkbox"/> | <input type="checkbox"/> | For hierarchical and complex designs, identification of the appropriate level for tests and full reporting of outcomes |
| <input checked="" type="checkbox"/> | <input type="checkbox"/> | Estimates of effect sizes (e.g. Cohen's d , Pearson's r), indicating how they were calculated |

Our web collection on [statistics for biologists](#) contains articles on many of the points above.

Software and code

Policy information about [availability of computer code](#)

Data collection No software was used to collect the data.

Data analysis All computer codes used in this study are available via GitHub at https://github.com/YueLi92/Contributions_CO2Phys_Def_SSP.

For manuscripts utilizing custom algorithms or software that are central to the research but not yet described in published literature, software must be made available to editors and reviewers. We strongly encourage code deposition in a community repository (e.g. GitHub). See the Nature Portfolio [guidelines for submitting code & software](#) for further information.

Data

Policy information about [availability of data](#)

All manuscripts must include a [data availability statement](#). This statement should provide the following information, where applicable:

- Accession codes, unique identifiers, or web links for publicly available datasets
- A description of any restrictions on data availability
- For clinical datasets or third party data, please ensure that the statement adheres to our [policy](#)

All CMIP6 simulations used in this study are publicly available at <https://esgf-node.llnl.gov/projects/cmip6/>. Atmospheric CO2 concentrations for future SSP scenarios were downloaded from <https://esgf-node.llnl.gov/projects/input4mips/>. Future land use datasets LUHv2f were downloaded from <https://luh.umd.edu/data.shtml>.

Human research participants

Policy information about [studies involving human research participants and Sex and Gender in Research](#).

Reporting on sex and gender

Population characteristics

Recruitment

Ethics oversight

Note that full information on the approval of the study protocol must also be provided in the manuscript.

Field-specific reporting

Please select the one below that is the best fit for your research. If you are not sure, read the appropriate sections before making your selection.

☐ Life sciences ☐ Behavioural & social sciences ☒ Ecological, evolutionary & environmental sciences

For a reference copy of the document with all sections, see [nature.com/documents/nr-reporting-summary-flat.pdf](https://www.nature.com/documents/nr-reporting-summary-flat.pdf)

Ecological, evolutionary & environmental sciences study design

All studies must disclose on these points even when the disclosure is negative.

Study description

Research sample

Sampling strategy

Data collection

Timing and spatial scale

Data exclusions

Reproducibility

Randomization

Blinding

Did the study involve field work? ☐ Yes ☒ No

Reporting for specific materials, systems and methods

We require information from authors about some types of materials, experimental systems and methods used in many studies. Here, indicate whether each material, system or method listed is relevant to your study. If you are not sure if a list item applies to your research, read the appropriate section before selecting a response.

Materials & experimental systems

n/a	Involved in the study
<input checked="" type="checkbox"/>	<input type="checkbox"/> Antibodies
<input checked="" type="checkbox"/>	<input type="checkbox"/> Eukaryotic cell lines
<input checked="" type="checkbox"/>	<input type="checkbox"/> Palaeontology and archaeology
<input checked="" type="checkbox"/>	<input type="checkbox"/> Animals and other organisms
<input checked="" type="checkbox"/>	<input type="checkbox"/> Clinical data
<input checked="" type="checkbox"/>	<input type="checkbox"/> Dual use research of concern

Methods

n/a	Involved in the study
<input checked="" type="checkbox"/>	<input type="checkbox"/> ChIP-seq
<input checked="" type="checkbox"/>	<input type="checkbox"/> Flow cytometry
<input checked="" type="checkbox"/>	<input type="checkbox"/> MRI-based neuroimaging